UNDERSTANDING INTENTIONS OF OTHERS REFLECTS EVOKED RESPONSES IN THE HUMAN MIRROR NEURON SYSTEM: EVIDENCE FROM COMBINED fMRI AND EEG REPETITION SUPPRESSION

Stephanie Ortigue*
Department of Psychology, Institute for Collaborative Biotechnologies, UCSB, Santa Barbara, CA, 93106

James C. Thompson, Raja Parasuraman
Department of Psychology, George Mason University, MSN 3F5, Fairfax, VA, 22030

Scott T. Grafton
Department of Psychology, UCSB Brain Imaging Center, Santa Barbara, CA, 93106

ABSTRACT

Viewing the behavior of other agents to infer and understand their intents recruits brain regions within the mirror neuron system (MNS), particularly the inferior parietal lobule and inferior frontal gyrus. However, decoding *when* intention understanding occurs in the human brain remains unclear. Accordingly, and to distinguish MNS involvement from lower level visual scene analysis, we tested repetition suppression effects in 24 healthy male volunteers who performed an intention inference task while their brain activity was recorded with high-spatial fMRI and high-temporal EEG recordings. During this intention inference task, participants were instructed to attend to video-clips displaying hand-on-object actions, and to try to decode "why" actions were being performed. Functional MRI results confirmed the specific role of the MNS and superior temporal sulcus (STS) in intention understanding by revealing repetition suppressions (RS) in inferior parietal, inferior frontal cortex, and STS when participants saw repeated actions with the same intention. High-density EEG neuroimaging combining brain microstate analysis with LAURA distributed linear source estimations expanded these results by revealing suppressed responses for intention decoding in this brain network in the early stage of processing (within the first 300 ms after the hand-on-object interaction). Together, these results establish that intention understanding is mediated by a specific subset of regions within the human MNS that are different than those used to decode lower level visual features related to the object. The findings identify a time window of activity within MNS that may be critical for intention decoding. This could potentially be used for on-line monitoring of action awareness.

1. INTRODUCTION

Understanding intentions of others is an essential component of social behavior. One of the neural systems that underlies computational processes needed to interpret actions and intentions of others is a network called the mirror neuron system (MNS; Figure 1). MNS includes a class of neurons with visuo-motor properties (i.e., mirror neurons) that are automatically activated both by the execution and the observation of object-related actions (Rizzolatti; Craighero 2004).
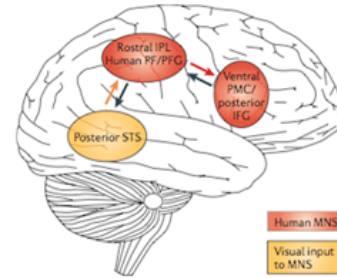

Fig.1., Shematic representation of the fronto-parietal MNS (red) and its main visual input from the superior temporal sulcus (STS, yellow) in the human brain. An anterior part of MNS is located in the inferior frontal gyrus (IFG) and adjacent ventral premotor cortex (PMC). A posterior part of MNS is located in the inferior parietal lobule (IPL), which can be considered the homologue area of area PF/PFG in the macaque. Adapted from Rizzolatti and Craighero, 2004.

Although MNS was originally found by responses of single neurons in the monkey (Rizzolatti; Craighero 2004), there is a growing body of evidence from non-invasive neurophysiological techniques and brain imaging studies that a similar MNS action observation-execution matching mechanism is also present in humans for action observation, execution, as well as in intention understanding (Grafton et al. 1996).
.

Although recruitment of the MNS is not a prerequisite to act or to understand the kinematics of an action, convergent evidence suggests that this fronto-parietal network is particularly important for the direct matching of actions, simulation, imitation and understanding hand-object interactions. It may also facilitate action and the decoding of intentions through top-down mechanisms from stored self-related motor experiences (Cross et al. 2008; Rizzolatti; Craighero 2004). The functional properties of MNS suggest that the

Report Documentation Page	*Form Approved* *OMB No. 0704-0188*

1. REPORT DATE **DEC 2008**	2. REPORT TYPE **N/A**	3. DATES COVERED **-**

4. TITLE AND SUBTITLE **Understanding Intentions Of Others Reflects Evoked Responses In The Human Mirror Neuron System: Evidence From Combined Fmri And Eeg Repetition Suppression**	5a. CONTRACT NUMBER
	5b. GRANT NUMBER
	5c. PROGRAM ELEMENT NUMBER
6. AUTHOR(S)	5d. PROJECT NUMBER
	5e. TASK NUMBER
	5f. WORK UNIT NUMBER
7. PERFORMING ORGANIZATION NAME(S) AND ADDRESS(ES) **Department of Psychology, Institute for Collaborative Biotechnologies, UCSB, Santa Barbara, CA, 93106**	8. PERFORMING ORGANIZATION REPORT NUMBER
9. SPONSORING/MONITORING AGENCY NAME(S) AND ADDRESS(ES)	10. SPONSOR/MONITOR'S ACRONYM(S)
	11. SPONSOR/MONITOR'S REPORT NUMBER(S)

12. DISTRIBUTION/AVAILABILITY STATEMENT
Approved for public release, distribution unlimited

13. SUPPLEMENTARY NOTES
See also ADM002187. Proceedings of the Army Science Conference (26th) Held in Orlando, Florida on 1-4 December 2008, The original document contains color images.

14. ABSTRACT

15. SUBJECT TERMS

16. SECURITY CLASSIFICATION OF:			17. LIMITATION OF ABSTRACT	18. NUMBER OF PAGES	19a. NAME OF RESPONSIBLE PERSON
a. REPORT **unclassified**	b. ABSTRACT **unclassified**	c. THIS PAGE **unclassified**	**UU**	**7**	

understanding of intentions of others may be based primarily on a mechanism that directly matches the sensory representation of the observed actions with one's own motor representations of those same actions; representations of past experiences that are stored and integrated at a higher-order cognitive level (Cross et al. 2008; Rizzolatti; Craighero 2004; Rizzolatti; Sinigaglia 2007). Support for a role of the MNS fronto–parietal network in human intention understanding comes from a growing body of neuroimaging observations from healthy volunteers that understanding of actions result in consistent recruitment of MNS (e.g., Cross et al. 2008; Grafton et al. 1996; Iacoboni et al. 2005). For instance, using a one-back paradigm that induces repetition suppression (RS) effects in response to observed actions and goals in fMRI, Hamilton and Grafton recently showed that MNS is involved in the decoding of goals exemplified by hand-object interactions and the involvement of the anterior intraparietal sulcus (aIPS). Notably this occurred in areas that are separable from those for decoding the observed movements or means to achieve an immediate goal (Grafton; Hamilton 2007). Using RS measures in response to observed videos showing novel vs. repeated kinematics; and novel vs. repeated immediate goals, Hamilton and Grafton could distinguish decoding related to different forms of action representation in the MNS. This defined a network that include the following nested functions: a visual component (visual analysis of muscle controls and then actions), a kinematic component (muscle control), an immediate goal component (reach and grasp control); and an (i.e., long-distance) agent's intention component in tasks such as opening or closing a box (goals and intentions; Figure 2; Grafton; Hamilton 2007; Hamilton; Grafton 2006).
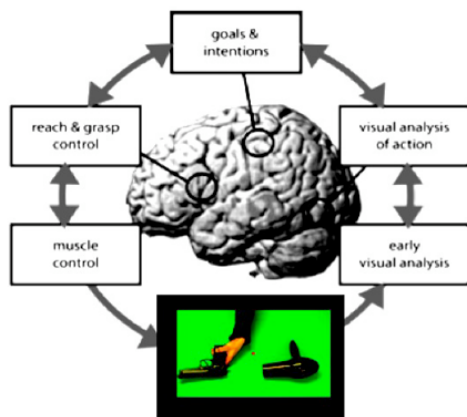

Fig. 2., Looped components of the visual-motor hierarchy. Adapted from Hamilton; Grafton 2007.

These findings do not necessarily imply that the change of activation in MNS is a direct consequence of an agent's intention ascription. The mere anticipation of a particular motor immediate goal (such as opening of a box) could be sufficient for the activation of MNS, and notably aIPS. Thus, the neural basis of intention understanding remains unresolved. One could wonder whether or not long-distant goals/intentions (i.e., to open a box to place screws inside) are represented in aIPS just as goals defined by simple hand-object interactions are. Does the capacity to understand the *why* of an action (intention) also involved the human fronto-parietal mirror network; and notably in aIPS? There is emerging evidence that inference of mental attribution and theory of mind may actually involve non MNS areas such as the superior temporal sulcus (Brass et al. 2007; de Lange et al. 2008; Thompson et al. 2005). If so, fMRI alone may not be adequate to fully characterize decoding processes due to the limited temporal resolution.

To answer these questions we conducted the present high-density visual event-related potentials (VEPs) and fMRI experiment in healthy human individuals while they were performing an intention inference task embedded in a one-back repetition paradigm known to induce repetition suppression effects in the human brain. The current study focuses on the temporal dynamics of action understanding at the level of hand-object interactions and the decoding of why an agent is grasping an object. This study is a prelude for characterizing the neural systems that underlie more complex behaviors, including actions performed in social contexts and between different agents. This next level is important for understanding mechanisms of corporation where understanding others intentions is crucial for achieving shared goals.

2. HYPOTHESIS

Based on the above, we predicted that brain regions involved in the understanding of intentions of others should show a greater response to novel intentions than to repeated intentions. Specifically, we predicted the inferior frontal and inferior parietal regions of the MNS to comprise a potential functional signature for intention representation. Because the right superior temporal sulcus (STS) has been associated with the observation of actions (Jellema et al. 2000), in particular unexpected actions and inferential processes (Brass et al. 2007; Saxe et al. 2004), it is also a possible locus for a intention representation.

3. MATERIAL AND METHODS

3.1. Population

Twenty-four male human subjects ranging from 19-42 yrs in age participated in the present study. All were right-handed with normal (or corrected) vision, and no psychiatric or neurological diseases, as ascertained with a detailed anamnesis. Participation was completely

voluntary. All gave their informed consent to take part in the study in accordance with the requirements of the local ethics board.

3.2. Procedure

We used repetition suppression in an event-related experiment to localize the spatio-temporal neural representation of intention understanding. Participants were asked to perform a motor intention inference task while the experimenter monitored their brain activity on a separate computer. This motor intention inference task was performed both in EEG and fMRI, i.e., two sessions a day apart from one another.

3.3. Stimuli material

A total of 32 sets of 3 second-long action video clips were generated. Each video clip depicted a hand reaching out to either transport or use an hair dryer or a gun (e.g., Figure 3). All video clips were created at George Mason University by filming intentional natural actions on an object. Controlled conditions were the following: visual field of action (left and right); position of the grip in space (under and over), hand of action (left and right). The wide variety of stimuli meant that we could be confident that the results revealed a general neural representation of intention understanding, rather than being an epiphenomenon of one particular type of video clip.

Fig. 3., Example video clip stimulus presented to the participant showing a hand reaching out to grasp the gun to use it.

3.4. Experimental design

Participants viewed sequences of video clips separated by a blank screen. In order to avoid any saccadic movements, a fixation red square remained constantly on the screen. After a sequence of eight video clips, a 6 s-long screen reminding the task instruction was systematically presented. Each sequence of eight movies began with a randomly chosen video clip designated as being novel. The subsequent video clips were chosen among the remaining set of video clips according to a pseudo-random order. Novel and repeated trials were defined in relation to the previous trial only, which meant that each individual video clip appeared in every condition. This means that all the conditions were perfectly balanced for all visual properties. Each participant completed five runs

with 8 sequences in each run, giving a total of 64 trials per run. Experimental blocks were intermixed for every participant. The same event-related design was used in both fMRI and EEG session. Inter-trial interval (ITI) varied in 2000 ms random increments from 2000 to 6000 ms.

3.5. Task Instruction

"In this experiment, you will be asked to look at a centred red square during the entire session while trying to guess the intention of the actor in every video clip (e.g., to use the object or to transport it)."

3.6. Data acquisition

Both functional and electrical neuroimaging was conducted at the UCSB Brain Imaging Center.

3.6.1. fMRI data acquisition

Functional MRI recordings were conducted using a 3T TIM Trio Siemens Magnetom with a 12 channel phased-array head coil. Foam padding was used for head stabilization. For each functional run, an echo planar gradient-echo imaging sequence sensitive to BOLD contrast was used to acquire 33 slices per repetition time (TR) (3 mm thickness), with a TR of 2000 ms, echo time (TE) of 30 ms, flip angle of 90 degrees, field of view (FOV) of 192 mm, and 64 x 64 matrix. Before all the functional runs, a high-resolution T1-weighted sagittal sequence image of the whole brain was acquired (TR = 15.0 ms; TE = 4.2 ms; flip angle = 9 degrees, 3-D acquisition, FOV = 256 mm; slice thickness = 0.89 mm, matrix = 256 x 256).

3.6.2. VEP data acquisition

Continuous electroencephalogram (EEG) was recorded from 128 AgCl carbon-fiber coated electrodes using an Electric Geodesic Sensor Net® (GSN300; Electrical Geodesic Inc., Oregon; http://www.egi.com/), where EEG electrodes are arrayed in a regular distribution across the head surface and the inter sensor distance is approximately 3 cm (Figure 4). The EEG was digitized at 500 Hz (corresponding to a sample bin of 2 ms), bandwidth at 0.01–200 Hz, with the vertex electrode (Cz) serving as an on-line recording reference; and impedances were kept below 50kΩ.

Fig. 4., High-density EGI sensor net.

3.7. Data analysis

3.7.1. fMRI data analyses

All fMRI analysis were carried out in SPM5 (www.fil.ion.ucl.ac.uk/spm). Data were realigned to correct for head movements. All realigned functional images were registered to the anatomical image. The anatomical images were then transformed to conform the Montreal National Institute (MNI) space and the parameters of this transformation were applied to the functional data and smoothed with an 8-mm full width half maximum filter. A design matrix was fitted for each subject with the trials in each cell of the 2x2x2x2x2 factorial design (intention types (to use or to transport); objects (gun or hairdryer); visual field of action (left and right); position of the grip in space (under and over), hand of action (left and right)) modeled by a standard hemodynamic response function and its temporal derivative. Each trial was modeled as a single event, starting at the onset of the grip. Rest was not modeled. The design matrix was fit to the data for each participant individually. After estimation, betas were taken to the second level for random effect analysis to identify which brain areas were preferentially activated novel intentions in comparison with repeated intentions (novel intentions > repeated intentions; Figure 5).

Fig. 5., Contrast of interest: novel intentions > repeated intentions.

3.7.2. EEG data analyses

EEG data were imported, averaged and analyzed in Cartool (version 3.32). Epochs of analysis were visually inspected for oculomotor (saccades, and blinks), muscles, and other artifacts in addition to an automated threshold rejection criterion of 100μV. After off-line artifact rejections, VEPs were computed covering 500 ms after the onset of grip. VEP data were then baseline corrected, and band-pass filtered between 1 and 30 Hz. VEP data were then recalculated off-line against the average reference, and normalized to their mean global field power (i.e., GFP) before group averaging. The GFP, computed as the spatial standard deviation of the scalp electric field, yields larger values for stronger electric fields and is calculated as the square root of the mean of the squared value recorded at each electrode (vs. the average reference). VEPs data from the novel and the repeated intention condition were then submitted to a brain microstate analysis (Lehmann 1987; Ortigue et al.

2004). To identify start and end of each optimal microstate, a standard pattern analysis previously described was employed using the grand-mean VEPs of each condition (Murray et al. 2008). This pattern analysis uses a hierarchical agglomerative cluster-algorithm to identify the predominant topographies (i.e., maps) and their sequence within a data set. The optimal number of maps (i.e., the minimal number of maps that best accounts for the data set) is determined based on a modified Krzanowski-Lai criterion (Krzanowski; Lai 1985). Importantly, this pattern analysis is reference-free, and insensitive to amplitude modulation of the same scalp potential field across conditions, since normalized maps are compared. It was performed across time and experimental conditions in order to determine whether and when novel versus repeated intentions engaged distinct configurations of intracranial generators. Then, the pattern of maps observed in the group-averaged data was statistically tested at the individual level using a competitive fitting procedure that determines whether a given experimental condition is more often described by one map versus another. Then, the extracted values of interest were subjected to a repeated measure ANOVA. Results were accepted as significant at P < 0.05. GFP were also statistically tested at the individual level using a Bonferroni corrected paired-test. Finally, intracranial sources of every significant brain microstate were estimated using the Local Auto-Regressive Average (LAURA) model of the unknown current density in the brain (Grave de Peralta Menendez et al. 2001). LAURA was used with a lead field (solution space) that was calculated on a realistic head model including 3005 solution points selected from a 6x6x6 mm grid equally distributed within the gray matter. Source estimations were rendered on the MNI/McGill average standard brain as supplied by Cartool. Then transformation between the MNI coordinate system and that of Talairach and Tournoux was performed with Cartool. Anatomical labeling was ascertained LONI.

4. RESULTS

3.1. Functional MRI results

Functional MRI results revealed RS in inferior parietal lobule, aIPS, STS and inferior frontal gyrus when participants saw repeated actions with the same intention (Figure 6-7). Other weaker activations were present in the superior frontal gyrus, pars opercularis and temporo-occipital region (Figure 6; Table 1).
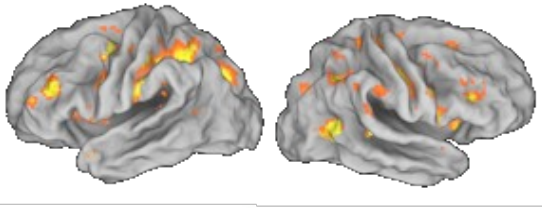
Fig. 6., fMRI BOLD responses obtained for all novel intentions> repeated intentions, shown on lateral views of the partially inflated left and right lateral surfaces of the PALS human brain from Caret v.5.51. All activations significant at the P < 0.001 level, uncorrected.

Table 1. Local Maxima in MNI coordinates of cerebral activations peaks for RS intentions

| Brain regions	Coordinates			Cluster size
	x	y	z	
Middle/Superior temporal sulcus	46	-61	11	104
Inferior frontal gyrus	-41	30	22	53
Pars opercularis	48	1	17	15
Superior frontal gyrus	-3	15	49	162
Superior frontal sulcus	-34	-14	55	61
Precentral gyrus	-50	6	30	18
aIPS	-32	-54	41	101
	38	-53	41	50
Supramarginal gyrus	-50	-32	45	67
Angular gyrus	32	-71	33	12
Central sulcus	42	-41	45	49
Temporo-occipital	-38	-74	10	29
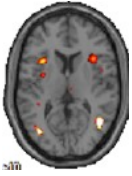
Fig. 7., fMRI BOLD responses obtained in the right superior temporal sulcus (46, -61, 11; x,y,z mm MNI coordinates) are shown in a transverse brain surface of MNI brain.

3.2. Electrophysiological results

High-density EEG neuroimaging, combining brain microstate analysis with LAURA distributed linear source estimations, expanded these above mentioned fMRI results by revealing the temporal dynamics of novel intentions as compared to repeated intentions. First, archetypal VEPs components (e.g., C1, P1 and N1) were readily observed in each condition (i.e., repeated intentions, novel intentions). Then, the microstate analysis identified four time periods of stability: Map 1: 0-60 ms; Map 2: 62-200 ms; Map 3: 202-380 ms; Map 4: 382-500 ms. One topography (Map 2; Figure 8) was present in the novel intentions condition only. LAURA source estimations of this brain topography demonstrated similarities between our VEP and fMRI data by showing right-lateralized activations including right STS (local maximum: posterior superior temporal sulcus: -48, -63, 15; x, y, z mm Talairach coordinates. Figure 8 displays brain horizontal sections showing the active cerebral areas for Map 2.
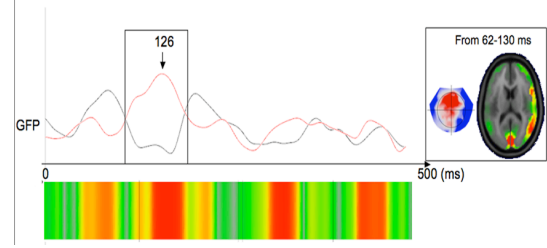

Fig. 8., Schematic representation of high-density electrical neuroimaging results. (Top row, left): GFP for novel intentions (in red) and repeated intentions (in black) across the collective 500 ms post-grip period. A significant difference peaking at 126 ms was observed for novel intentions in comparison with repeated intentions. (Bottom row): Results of the Bonferroni corrected paired t-test for GFP. Color scale indicates the threshold of p values (green > 0.05; red < 0.05). (Top row, right): Topography of the Map 2 is shown with the nasion upward and left scalp leftward. Blue areas depict negative potentials and red areas depict positive potentials. Intracranial brain generators of Map 2 as estimated with LAURA inverse solution.

Map 2's temporal window was also characterized by a significant difference of global field power (GFP) between novel intentions (in red in Figure 8) and repeated intentions (in black in Figure 8). Group-averaged data revealed a GFP peak at 126 ms for novel intentions, although GFP for repeated intentions was almost extinguished at the same time period. The reliability of this microstate at the group-averaged level was confirmed at the individual level using a Bonferroni corrected paired Ttest on GFP (Figure 8, color scale on the bottom row). More precisely, this paired Ttest revealed the following GFP differences: From 118 ms to 138 ms, with a peak at 126 ms (t= 2.71; p=0.013); From 238 ms to 250 ms with a peak at 246 ms (t=2.54; p=0.02), both in favor of novel intentions.

5. DISCUSSION

Combining event-related fMRI and EEG recordings, we confirmed the effectiveness of repetition suppression to assess the neural bases of intention understanding in the human brain. This reinforces previous data (Grafton; Hamilton 2007; Hamilton; Grafton 2008; Hamilton et al. 2006) that showed the possibility of using RS to study a much wider range of functions than examined previously (Naccache; Dehaene 2001). Our results demonstrate a robust RS for intention understanding. These data have two important implications.

First, we demonstrate that intention understanding is mediated by a specific subset of regions within both the human MNS and the superior temporal

5

sulcus. This network is different than the network for decoding lower level visual features related to the object or how a hand moves. Critically, we showed a systematic reduction of activation in inferior frontal gyrus, inferior parietal lobule, aIPS, and STS following the repetition of an intention relative to a novel intention. Thus our findings reinforce previous work showing activation of IPL and IPS for hand action observation (Grèzes; Decety 2001) and immediate goal representation. Critically, the present RS on aIPS, a brain area known to be crucial for on-line control of movements within the first 100 ms of goal-dependent reach-to-grasp actions (Frey et al. 2005; Tunik et al. 2005), suggests that observed immediate goals may reflect the maintenance of a more distant goal representation from one trial to the next. Along these lines, we assume the decoding of intentions might vary as a function of the type of grasps. Further investigations need to be done to unravel the functional dynamics of intention understanding with aIPS. The second key result from the current study is RS for intention in the STS, a core area in inferential processes. This reinforces its critical role in action interpretation (Brass et al. 2007; de Lange et al. 2008; Jellema et al. 2000). Thus, our data strongly support a combined mirroring and inference-based account of intention understanding (Keysers; Gazzola 2007).

Our electrical neuroimaging findings identify the temporal dynamics of intention understanding by demonstrating a two-step RS mechanism across the collective 500 ms after grip onset. First, we showed an early RS effect between 62 and 130 ms after grip onset; and also a later one around 246 ms. This suggests, that when observing actions done by others, individuals may understand the *why* of an action (e.g., to hold a gun to shoot) in the early stage of visual processing (within the first 300 ms). This is in line with previous work demonstrating that RS can emerge as early as 75 ms after stimulus onset (Desimone 1996); at 160 ms (Henson; Rugg 2003) and then around 300 ms. Although the first component is often assumed to call for perceptual accounts, the second component is assumed to call for higher-order cognitive mechanisms, such as semantic memory (Guo et al. 2007; Henson; Rugg 2003). Our LAURA source estimations reinforces this latter assumption by showing modulation of activity in associative areas (e.g., STS, IPL) in the first stage of visual processing. Although the standard functional model of visual system often assumed that information processing occurs in a feed-forward manner between hierarchically arranged cortical areas, suggesting that neurons in lower brain areas might have shorter response latencies to visual stimuli than those in higher-order brain areas, recent electrophysiological evidence from both animal and human studies argue for a bidirectional mechanism (e.g., Bullier 2001). Neurons in several higher-order cortical areas (e.g., parietal lobe) can respond, for instance, as early as 120–160 ms after stimulus onset (Bullier 2001). Early visual evoked potentials (VEPs) are thus not exclusively generated by sensory activation but also by higher-order integrative brain areas. Thus, our VEP data suggests that: i) complex visual analysis of action and intention understanding, implicating brain areas within and beyond the visual cortex, may occur within the first 300 ms after grip onset; and that ii) cognitive processes can be initiated (if not entirely completed) within this short temporal window. Thus, our findings support the hypothesis that cognitive processing related to goal representations may occur much faster than previously thought (Tunik et al. 2005).

CONCLUSIONS

Our results complement recent studies of decoding intentionality (de Lange et al. 2008; Fogassi et al. 2005; Hamilton; Grafton 2006; Hamilton; Grafton 2008) and suggest that the network including aIPS, inferior frontal gyrus and STS plays a central role in interpreting the goals of observed hand actions. We hypothesize that this network is part of a more general system for inferring action intentions for agents independent of objects. If so, this approach could be used to study actions between individuals as they attempt to decode shared intentions.

ACKNOWLEDGEMENTS

REFERENCES

Brass, M., R. M. Schmitt, S. Spengler, and G. Gergely, 2007: Investigating action understanding: inferential processes versus action simulation. *Curr Biol*, **17,** 2117-2121.

Bullier, J., 2001: Integrated model of visual processing. *Brain Res Brain Res Rev*, **36,** 96-107.

Cross, E., D. Kraemer, A. Hamilton, W. Kelley, and S. Grafton, 2008: Sensitivity of the Action Observation Network to Physical and Observational Learning. *Cerebral Cortex*, 12.

de Lange, F. P., M. Spronk, R. M. Willems, I. Toni, and H. Bekkering, 2008: Complementary systems for understanding action intentions. *Curr Biol*, **18,** 454-457.

Desimone, R., 1996: Neural mechanisms for

visual memory and their role in attention. *Proc Natl Acad Sci U S A*, **93,** 13494-13499.

Fogassi, L., P. F. Ferrari, B. Gesierich, S. Rozzi, F. Chersi, and G. Rizzolatti, 2005: Parietal lobe: from action organization to intention understanding. *Science*, **308,** 662-667.

Frey, S. H., D. Vinton, -. N. Newman, R.N., and S. T. Grafton, 2005: Cortical topography of human anterior intraparietal cortex active during visually-guided grasping. *Cognitive Brain Research*, **23,** 397-405.

Grafton, S. T., and A. F. Hamilton, 2007: Evidence for a distributed hierarchy of action representation in the brain. *Hum Mov Sci*, **26,** 590-616.

Grafton, S. T., M. A. Arbib, L. Fadiga, and G. Rizzolatti, 1996: Localization of grasp representations in humans by positron emission tomography. 2. Observation compared with imagination. *Exp Brain Res*, **112,** 103-111.

Grave de Peralta Menendez, R., S. Gonzalez Andino, G. Lantz, C. M. Michel, and T. Landis, 2001: Noninvasive localization of electromagnetic epileptic activity. I. Method descriptions and simulations. *Brain Topogr*, **14,** 131-137.

Grèzes, J., and J. Decety, 2001: Functional anatomy of execution, mental simulation, observation, and verb generation of actions: a meta-analysis. *Human brain mapping*, **12,** 1-19.

Guo, C., A. L. Lawson, and Y. Jiang, 2007: Distinct neural mechanisms for repetition effects of visual objects. *Neuroscience*, **149,** 747-759.

Hamilton, A. F., and S. T. Grafton, 2006: Goal representation in human anterior intraparietal sulcus. *J Neurosci*, **26,**

Hamilton, A. F. d. C., and S. T. Grafton, 2008: Action outcomes are represented in human inferior frontoparietal cortex. *Cereb Cortex*, **18,** 1160-1168.

Hamilton, A. F. d. C., D. M. Wolpert, U. Frith, and S. T. Grafton, 2006: Where does your own action influence your perception of another person's action in the brain? *Neuroimage*, **29,** 524-535.

Henson, R. N., and M. D. Rugg, 2003: Neural response suppression, haemodynamic repetition effects, and behavioural priming. *Neuropsychologia*, **41,** 263-270.

Iacoboni, M., I. Molnar-Szakacs, V. Gallese, G. Buccino, J. C. Mazziotta, and G. Rizzolatti, 2005: Grasping the intentions of others with one's own mirror neuron system. *PLoS Biol*, **3,** e79.

Jellema, T., C. I. Baker, B. Wicker, and D. I. Perrett, 2000: Neural representation for the perception of the intentionality of actions. *Brain Cogn*, **44,** 280-302.

Keysers, C., and V. Gazzola, 2007: Integrating simulation and theory of mind: from self to social cognition. *Trends Cogn Sci (Regul Ed)*, **11,** 194-196.

Krzanowski, W., and Y. T. Lai, 1985: A criterion for determining the number of groups in a data set using sum of squares clustering. *Biometrics*, **44,** 23-34.

Lehmann, D., 1987: Principles of spatial analysis. *Handbook of electroencephalography and clinical neurophysiology, vol. 1. Methods of analysis of brain electrical and magnetic signals*, A. S. Gevins, and A. Re mond, Eds., Elsevier, 309-354.

Murray, M. M., D. Brunet, and C. M. Michel, 2008: Topographic ERP analyses: a step-by-step tutorial review. *Brain Topogr.*, **20,** 249-264.

Naccache, L., and S. Dehaene, 2001: Unconscious semantic priming extends to novel unseen stimuli. *Cognition*, **80,** 215-229.

Ortigue, S., C. M. Michel, M. M. Murray, C. Mohr, S. Carbonnel, and T. Landis, 2004: Electrical neuroimaging reveals early generator modulation to emotional words. *Neuroimage*, **21,** 1242-1251.

Rizzolatti, G., and L. Craighero, 2004: The mirror-neuron system. *Annu Rev Neurosci*, **27,** 169-192.

Rizzolatti, G., and C. Sinigaglia, 2007: Mirror Neurons and Motor Intentionality. *Funct Neurol*, **22,** 205-210.

Saxe, R., D. K. Xiao, G. Kovacs, D. I. Perrett, and N. Kanwisher, 2004: A region of right posterior superior temporal sulcus responds to observed intentional actions. *Neuropsychologia*, **42,** 1435-1446.

Thompson, J. C., M. Clarke, T. Stewart, and A. Puce, 2005: Configural processing of biological motion in human superior temporal sulcus. *J Neurosci*, **25,** 9059-9066.

Tunik, E., S. H. Frey, and S. T. Grafton, 2005: Virtual lesions of the anterior intraparietal area disrupt goal-dependent on-line adjustments of grasp. *Nat Neurosci*, **8,** 505-511.